

Experimental and theoretical investigations of the responsivity of field effect transistors based Terahertz detectors versus substrate thickness

D. Coquillat¹, J. Marczewski², P. Kopyt³, N. Dyakonova¹, S. Ruffenach¹, D. But¹, F. Teppe¹,
F. Schuster^{1,4}, B. Giffard⁴ and W. Knap¹

¹Laboratoire Charles Coulomb (L2C), UMR 5221 CNRS-Université de Montpellier, Montpellier, France

²Institute of Electron Technology, Al. Lotnikow 32/46, 02-668 Warsaw, Poland

³Institute of Radioelectronics, ul. Nowowiejska 15/19, 00-665 Warsaw, Poland

⁴CEA-Leti MINATEC, 17 rue des Martyrs, Grenoble, France

Abstract— Phenomena of the radiation coupling to the field effect transistors based terahertz detectors is studied. We show that in the case of flat metallic antennas important part of radiation, instead coupling to the transistors, is coupled to the substrate leading to losses. Experimental and theoretical investigations of the responsivity versus substrate thickness are performed. They clearly show how to minimize the losses by the detector substrate thinning.

I. INTRODUCTION

ONE of the big problems of the terahertz (THz) detectors comes from the fact that incoming energy of the radiation is penetrating into the substrate. The THz radiation may be lost or may be re-directed to other detectors (cross-talk effects). The substrate with metalized back-plane becomes a dielectric waveguide. Because the modes propagating in such a waveguide are only weakly attenuated, they may become one of the loss mechanisms responsible for diminished responsivity of any detecting circuit fabricated on such a substrate [1].

One of the solutions to avoid this problem is thinning the detector substrate. One may expect that in sufficiently thin substrate the effects of THz radiation propagation and losses will be diminished. In this paper Si MOSFET-based THz detectors were fabricated [2, 3], thinned by grinding, and measured using sub-THz radiation source operating in the bandwidth 265–375 GHz [4]. A careful analysis of the dielectric waveguide modes propagating in the substrate of different thickness and that affect the performance of the antenna is presented.

II. RESULTS

The detector consisted of a n-MOSFET as rectifying device integrated with a bow-tie antenna connected to the source and the gate terminals (radius 120 μm for an angle of 120°) as shown in the inset of Fig. 1. To study the effects related to energy lost in the substrate beneath the antenna, four identical chips containing a detector designed for 300 GHz were thinned to tens of microns by grinding (in the range 125 μm –55 μm). For frequency responsivity measurements, the detectors were biased at a gate voltage close to the threshold voltage. The measured responsivity of the detector is defined as the ratio between the photoresponse and the radiation power impinging on the active area of the device. The responsivity shown in Fig. 1 reveals a strong dependence on Si substrate thickness. When the substrates modes are reduced using a

thinned substrate, the peak responsivity at ~ 280 GHz shows a more than 10-fold increase of the responsivity of the 55- μm thick chip as compared with the 125- μm thick chip. Thanks to using this thinning process, measured responsivities as high as 600 V/W around 285 GHz have been achieved.

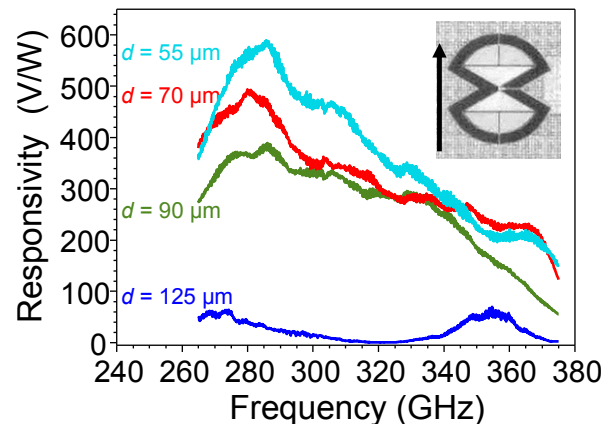


Fig. 1. Influence of thinning silicon substrate on n-MOSFET detector measured responsivity as a function of the frequency of the incident radiation. The inset shows a photo of the transistor integrated with antenna.

III. DISCUSSION

Let us discuss closer the loss mechanisms due to the propagation in the substrate and responsible for diminished responsivity. The electromagnetic (EM) analysis of the sample including a bow-tie antenna integrated with an active device and fabricated on a substrate. EM calculations require a numerical full-wave approach. To this end, a 3-dimensional (3D) model of the structure was created and solved using the finite difference time domain (FDTD) algorithm implemented in the QuickWave 3D environment [6].

The first version of the 3D model consisted of a grounded infinite slab of lossless silicon with thickness d , with a bow-tie antenna printed on the top surface [4]. The planar antenna printed on a dielectric slab launches not only the plane wave propagating away from the structure, but also the substrate waves. This effect can be analyzed by numerically calculating the portion of the power propagating away from the antenna and contained in the substrate only [4]. The results obtained at the frequency 300 GHz are shown in Fig. 2. The more power propagates in the substrate, the lower becomes efficiency of the radiator at emitting (or receiving) the plane wave into the air.

A comparison of the curves obtained numerically for the antenna and those derived analytically for consecutive substrate modes reveals that the planar structures is quite

effective at launching the waveguide modes into the substrate. For low values of d , the portion of the power emitted into the dielectric by the bow-tie follows exactly the predictions for the TM_0 mode.

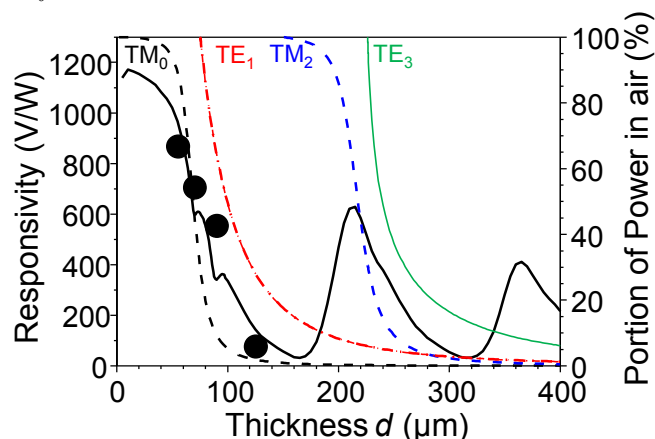


Fig. 2. EM modes TM_0 , TE_1 , TM_2 , and TE_3 supported in grounded dielectric waveguide. The solid black curve illustrates the portion of the power contained in air obtained by numerical integration of the Poynting vector over a surface located above the bow-tie antenna - thus only the waves that propagates along the vector normal to the chip top surface is accounted for [4]. The circles mark the measurement points corresponding to the maximum of responsivity (for read-out circuit with infinite impedance).

The point $d \sim 76.6 \mu\text{m}$, is the threshold thickness at which the TE_1 mode can exist (at 300 GHz). The total power launched into the dielectric by the bow-tie splits, because a part of it couples to the TM_0 mode, and the other part couples to the TE_1 mode. While for the TM_0 mode a slab of $d = 76.6 \mu\text{m}$ is relatively thick resulting in significant portion of the mode power propagating in the substrate, for the TE_1 mode it is electrically thin meaning that nearly all of the power that couples into that mode propagates in air. Thus, the total power in the substrate is reduced, which explains the slower rise of the bow-tie curve in the area. A similar effect occurs for d larger than $153 \mu\text{m}$, which is the threshold thickness for the TM_2 mode. Now, the power launched by the bow-tie couples to as many as three substrate modes, with the TM_2 mode initially propagating mostly in air. The behavior of this mode results in a significant reduction of total power observed in the substrate for the bow-tie antenna and for relatively wide range of d reaching up to the threshold thickness of the next mode – TE_3 – where the cycle repeats.

The existing numerical model can, thus, be safely extended to account for finite dimensions of the silicon substrate. To this end, one more 3D model was prepared. It contains a single bow-tie antenna located on a lossy ($10 \Omega\text{cm}$) silicon chip of dimensions $2.25 \text{ mm} \times 2.20 \text{ mm}$ positioned on a ground plane. The sample was illuminated with plane wave propagating along the vector normal to the sample top surface. The wave was polarized along the vertical axis of the bow-tie. In the numerical model, the antenna was loaded with lumped impedance equal to the input impedance of a typical n-MOSFET fabricated in the 130 nm CMOS process. The results obtained with this approach turned out to be consistent with an alternative formulation described in Ref. 7, hence only one set of results are presented in Fig. 3 for different thicknesses of the chip.

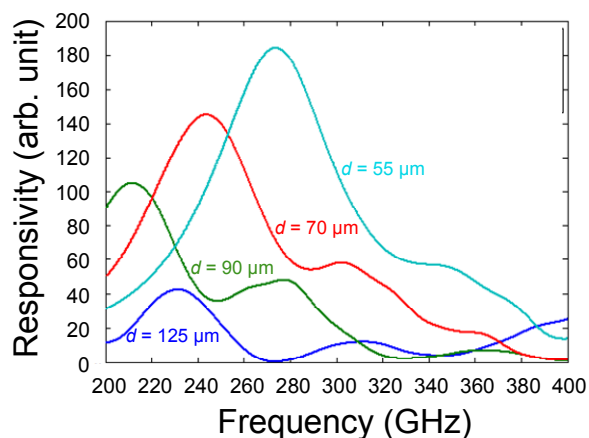


Fig. 3. The responsivity of the chip versus frequency as predicted by the 3D numerical model for several thicknesses of the chip.

The overall trend is consistent with the predictions based on the analysis of the substrate modes, with smaller thicknesses of the chip contributing to an increase of the observed responsivity. The peak responsivity predicted at $\sim 280 \text{ GHz}$ agrees well with the measurements similarly to more than 10-fold reduction of responsivity of the $125 \mu\text{m}$ -thick chip as compared to the thinnest variant. The differences between the predictions and the measurements can be attributed to: i) no glue layer in the model; ii) no fill metallization in the vicinity of the antenna; iii) no wire-bonds surrounding the chip and contributing to the overall responsivity at larger thicknesses.

Acknowledgments: We acknowledge funding from the ANR P2N NADIA (ANR-13-NANO-0008), the IMPAD imaging project from the French Government Defense procurement and technology agency DGA, the COST Action MP1204 TERA-MIR, the PHC Polonium, the National Centre for Research & Development in Poland (grant PBS1/A9/11/2012), the Polish National Science Centre (Grant UMO-2012/05/B/ST7/02112), the Laboratoire International Associé “TERAMIR”, and the project HARMONIA.

REFERENCES

1. D. M. Pozar, “Considerations for Millimeter Wave Printed Antennas”, *IEEE Trans. on Antennas and Propagation* 31(5), 740–747 (1983).
2. F. Schuster, D. Coquillat, H. Videlier, M. Sakowicz, F. Teppe, L. Dussopt, B. Giffard, T. Skotnicki, and W. Knap, “Broadband THz imaging with highly sensitive silicon CMOS detectors,” *Opt. Express* 19(8), 7827–7832 (2011).
3. W. Knap, S. Nadar, H. Videlier, S. Boubanga-Tombet, D. Coquillat, N. Dyakonova, F. Teppe, K. Karpierz, J. Lusakowski, M. Sakowicz, *et al.*, “Field Effect Transistors for Terahertz Detection and Emission,” *J. Infrared Milli. Terahertz Waves* 32(5), 618–628 (2011).
4. D. Coquillat, J. Marczewski P. Kopyt, N. Dyakonova, B. Giffard, W. Knap, “Improvement of terahertz field effect transistor detectors by substrate thinning and radiation losses reduction”, submitted (2015).
5. R. E. Collin, “Field Theory of Guided Waves”, McGraw-Hill, 470 (1960).
6. W. K. Gwarek, M. Celuch, M. Sypniewski, A. Wieckowski, “QuickWave-3D Manual v.2015,” QWED, Poland (2015).
7. PK5 P. Kopyt, P. Zagrajek, J. Marczewski, K. Kucharski, B. Salski, J. Lusakowski, W. Knap, W. K. Gwarek, “Analysis of Sub-THz Radiation Detector Built of Planar Antenna Integrated with MOSFET,” *Microelectronics Journal* 45, 1168–1176 (2014).